Stem Cell Reports
Article

OPEN ACCESS

An hPSC-Derived Tissue-Resident Macrophage Model Reveals Differential Responses of Macrophages to ZIKV and DENV Infection

Jianshe Lang,[1] Yichen Cheng,[1] Alyssa Rolfe,[2] Christy Hammack,[1] Daniel Vera,[3] Kathleen Kyle,[3] Jingying Wang,[2] Torsten B. Meissner,[4] Yi Ren,[2] Chad Cowan,[4] and Hengli Tang[1,*]

[1]Department of Biological Science, Florida State University, 319 Stadium Dr., Tallahassee, FL 32306-4295, USA
[2]Department of Biomedical Sciences, College of Medicine, Florida State University, Tallahassee, FL 32304, USA
[3]Center for Genomics and Personalized Medicine, Department of Biological Science, Florida State University, Tallahassee, FL 32306, USA
[4]Department of Stem Cell and Regenerative Biology and Harvard Stem Cell Institute, Harvard University, Cambridge, MA 02138, USA
*Correspondence: tang@bio.fsu.edu
https://doi.org/10.1016/j.stemcr.2018.06.006

SUMMARY

Zika virus (ZIKV) and dengue virus (DENV) are two closely related flaviviruses that lead to different clinical outcomes. The mechanism for the distinct pathogenesis of ZIKV and DENV is poorly understood. Here, we investigate ZIKV and DENV infection of macrophages using a human pluripotent stem cell (hPSC)-derived macrophage model and discover key virus-specific responses. ZIKV and DENV productively infect hPSC-derived macrophages. DENV, but not ZIKV, infection of macrophages strongly activates macrophage migration inhibitory factor (MIF) secretion and decreases macrophage migration. Neutralization of MIF leads to improved migratory ability of DENV-infected macrophages. In contrast, ZIKV-infected macrophages exhibit prolonged migration and express low levels of pro-inflammatory cytokines and chemokines. Mechanistically, ZIKV disrupts the nuclear factor κB (NF-κB)-MIF positive feedback loop by inhibiting the NF-κB signaling pathway. Our results demonstrate the utility of hPSC-derived macrophages in infectious disease modeling and suggest that the distinct impact of ZIKV and DENV on macrophage immune response may underlie different pathogenesis of Zika and dengue diseases.

INTRODUCTION

As one of the most widespread mosquito-borne flaviviruses, dengue virus (DENV) causes millions of dengue disease cases worldwide each year. Dengue diseases include dengue fever and the more severe dengue hemorrhagic fever or dengue shock syndrome (Halstead, 2007). It is commonly held that increased pro-inflammatory cytokines and chemokines induced by DENV constitute a "cytokine storm" that results in vascular permeability in patients with dengue hemorrhagic fever.

Zika virus (ZIKV), also a mosquito-transmitted flavivirus, has been identified as the pathogenic agent of the 2015 Brazilian epidemic of fetal microcephaly (Rasmussen et al., 2016; Miner and Diamond, 2017). In a majority of cases, ZIKV infection of adults is asymptomatic or only results in mild symptoms. However, more severe neurological conditions such as Guillain-Barré syndrome may occur in rare cases. ZIKV infection of women during pregnancy is a major concern, as this can lead to fetal microcephaly and intrauterine growth restriction (Rasmussen et al., 2016; Miner and Diamond, 2017; Kass and Merlino, 2016). Clinical reports and experimental data have shown that ZIKV can infect fetal and adult neural stem cells (Li et al., 2016; Mlakar et al., 2016; Tang et al., 2016), damage testis (Ma et al., 2016; Govero et al., 2016), and transmit sexually (Moreira et al., 2017), suggesting that the virus has likely developed strategies for crossing a number of physiological barriers, including the placental barrier, and possibly the blood-brain and blood-testis barriers as well. Despite being similar to ZIKV in both genome organization and geographic distribution, DENV has not been associated with trans-placental infection of fetuses in the decades of clinical observation (Halstead, 2007). Conversely, ZIKV has not been reported to cause hemorrhagic fever or shock syndrome even though it was discovered seven decades ago (Rasmussen et al., 2016; Miner and Diamond, 2017; Kass and Merlino, 2016).

Macrophages are one of the important cell types involved in dengue pathogenesis (Halstead, 2007). ZIKV has recently been reported to infect primary human placenta-specific macrophages, Hofbauer cells (Quicke et al., 2016; Jurado et al., 2016), which are derived from villous mesenchymal stem cells early in pregnancy and from the recruited fetal monocytes later in pregnancy (Castellucci et al., 2000). ZIKV also infects decidual macrophages (Costa et al., 2016), which are specialized cells present in the maternal decidual tissue and play an immunosuppressive role in pregnancy to prevent rejection of the fetus (Heikkinen et al., 2003; Lidstrom et al., 2003; Gustafsson et al., 2008). However, the role of macrophages in ZIKV infection of healthy adults remains unclear. Tissue-resident macrophages are present throughout the body and derived from two distinct origins. The majority of resident macrophages in the healthy tissues are derived from yolk sac before the establishment of the blood circulation. Circulating monocytes can also be recruited into the tissues to replenish tissue macrophages under homeostatic and

pathological conditions (Varol et al., 2015; Perdiguero and Geissmann, 2016).

Primary human monocyte-derived macrophages are a physiologically relevant cell model for studying blood-borne pathogens, but supply and donor variability are common issues. The isolation of yolk sac-derived tissue-resident macrophages poses an even more considerable technical challenge. Alternative approaches to model these macrophages will be of great value for studying macrophage-pathogen interactions.

Recent progress in stem cell research has opened up a new avenue for human disease modeling, including ZIKV infection (Tang et al., 2016). In the current study, we apply human pluripotent stem cell (hPSC)-derived macrophages, which have been shown to developmentally resemble yolk sac-derived tissue-resident macrophages (Vanhee et al., 2015; Buchrieser et al., 2017), to investigate the role of human macrophages in ZIKV and DENV pathogenesis. We found that the infected macrophages exhibit differential responses to ZIKV and DENV, which provide a possible explanation for ZIKV persistence and dissemination in human tissues.

RESULTS

hPSC-Derived Macrophages Support Productive ZIKV and DENV Infection

We first determined whether primary human monocyte-derived macrophages are permissive to ZIKV and DENV infection *in vitro*. We observed that human adult monocyte (Figures S1A–S1D)-derived macrophages (Figure S1E) supported productive infection of DENV and two strains of ZIKV, an African strain MR766 ($ZIKV^{M}$), and a clinical isolate PRVABC59 ($ZIKV^{PR}$) from the 2015 Zika outbreak in Puerto Rico, with different cell size changes (Figures S1F and S1G), similar infection rates (Figures S1H–S1J), and low levels of cell death (Figures S2A–S2E).

We next generated macrophages from hPSCs, including human embryonic stem cells (hESCs) and human induced pluripotent stem cells (hiPSCs), to model ZIKV and DENV infection of yolk sac-derived tissue-resident macrophages. Both hESCs and hiPSCs were maintained in an undifferentiated state with high expression of the pluripotency markers, including *SOX2*, *OCT4*, and *SSEA4* (Figure 1A). To initiate differentiation, hPSCs were cultured in suspension to form spherical embryoid bodies (EBs) for 5–7 days (Figures 1B and 1C). Then large EBs were transferred into gelatin-coated plates and further differentiated by macrophage colony-stimulating factor 1 (CSF1) and interleukin-3 (IL-3). After around 15 days, the round-shaped monocyte-like cells were continuously released from the flatten EBs and suspended in the medium (Figures 1B and 1C). Monocyte-like cells collected from the culture medium supernatant were further differentiated into macrophages in the presence of CSF1 (Figures 1B and 1C). RNA sequencing results revealed that these cells highly expressed the defined markers of the mononuclear phagocyte system, including *CD163*, *CSF1R*, *CD68*, *SPI1* (*PU-1*), *CD4*, *CD14*, *CD163*, etc. (Figure 1D). Further analysis of the expressions of *CD14*, *CD163*, *CD11b*, and *CD68* by flow cytometry and immunostaining indicated the high purity of the differentiated macrophages (Figures 1E and 1F). In contrast to hPSCs, the resulting macrophages were able to ingest myelin debris isolated from the mouse brains, indicating that the hPSC-derived macrophages have the phagocytic capacity (Figures 2A and 2B). Furthermore, hPSC-derived macrophages secreted high levels of pro-inflammatory cytokine tumor necrosis factor alpha (TNF-α), C-C motif chemokine ligand 4 (CCL4), and C-X-C motif chemokine ligand 8 (CXCL8/IL-8) in response to lipopolysaccharide (LPS) stimulation with significant morphological change (Figures 2C–2E). To further test whether the innate immune programs are functional in hPSC- and primary human monocyte-derived macrophages, we treated these cells with LPS or poly(I:C) to activate Toll-like receptor 4 (TLR4) and the antiviral pattern recognition receptors TLR3 and RIG-I/MDA5, respectively. As shown in Figure 2F, the transcription of interferon-stimulated genes *MX1*, *IFI44*, *RSAD2*, and *OASL*, and pro-inflammatory cytokines IL-6 (*IL6*) and *TNF*, were strongly induced by LPS and poly(I:C), suggesting that antimicrobial signaling pathways are intact in these cells. Together, these data suggest that hPSCs are successfully differentiated into functional macrophages.

We next infected hPSC-derived macrophages with ZIKV and DENV. Similar to primary human monocyte-derived macrophages, both hESC- and hiPSC-derived macrophages increased in cell size after exposure to DENV, compared with ZIKV exposure or mock treatment (Figure 3A). These macrophages were infected by both viruses with around 90% infection rate (Figures 3B and 3C). Furthermore, the continuous release of virus particles into the culture medium suggested the persistent and productive ZIKV and DENV infection of hPSC-derived macrophages (Figure 3D). Both ZIKV and DENV infections also responded to the treatment by two previously identified anti-ZIKV drugs (Xu et al., 2016) (Figure 3E). Little to no infection was detected in hESCs and hiPSCs exposed to DENV or ZIKV with the same MOI (MOI = 10) (Figures S3A and S3B).

ZIKV and DENV Infection Result in Different Migratory Capacity of Macrophages

Macrophages are able to migrate within the tissues and this mobility may facilitate virus dissemination and barrier crossing. To explore the effect of DENV or ZIKV infection on macrophage migration, we performed a wound-healing

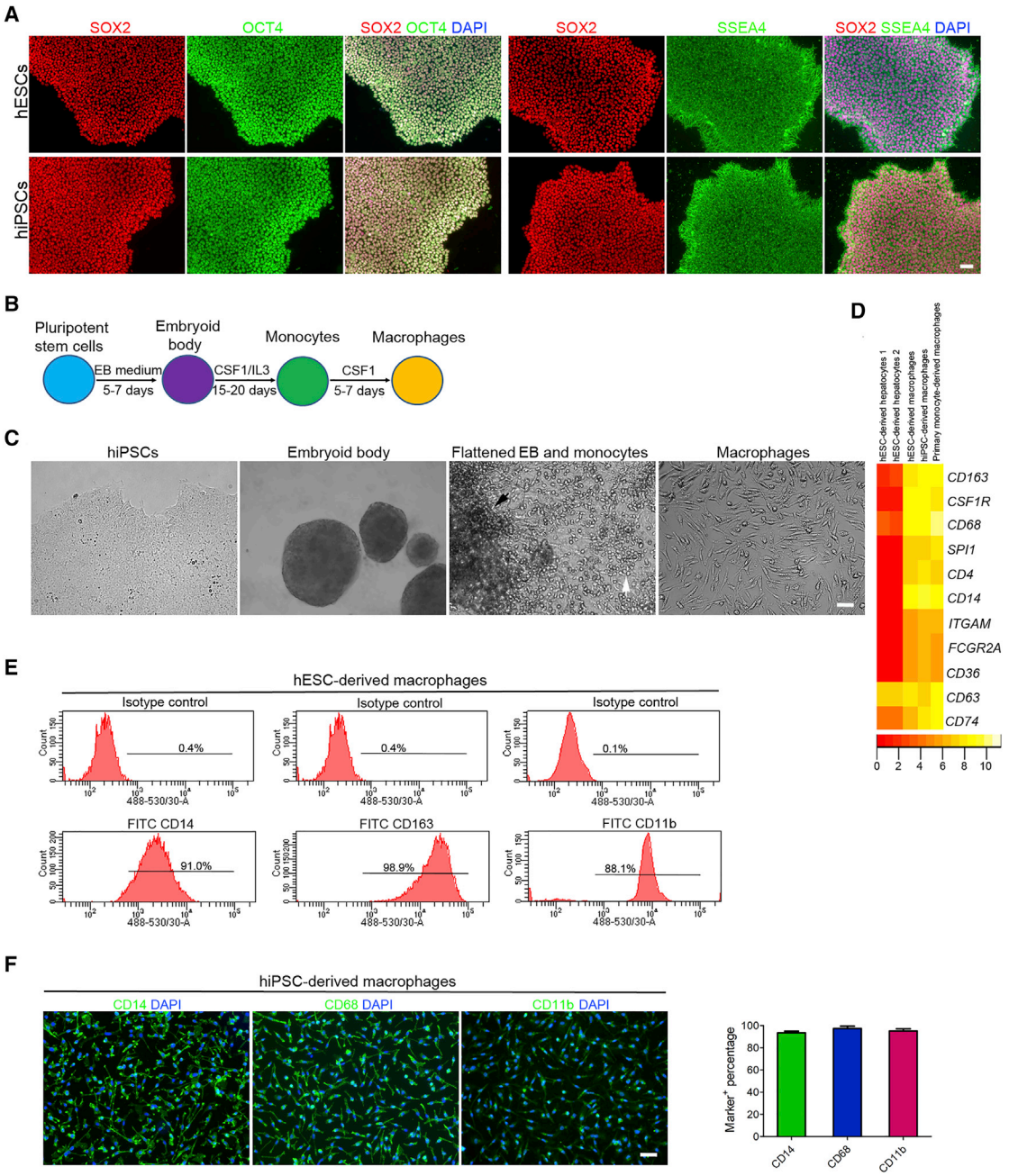

Figure 1. Directed Differentiation of Human Pluripotent Stem Cells into Macrophages

(A) Immunostaining images of hESCs and hiPSCs showing the high expression of pluripotent markers *SOX2*, *OCT4*, and *SSEA4*. Scale bar, 50 μm.

(B) Schematic diagram of macrophage differentiation from human pluripotent stem cells.

(C) Phase contrast microscopy images of hiPSCs, embryoid bodies (EBs) formed from hiPSCs, flattened EBs (indicated with the black arrowhead), the surrounding monocytes (indicated with the white arrowhead), and macrophages at day 5. Scale bar, 50 μm.

(D) Heatmap of the defined macrophage markers generated from the RNA sequencing analysis of primary human monocyte- and hPSC-derived macrophages and hESC-derived hepatocytes.

(E) Flow cytometry analysis of *CD14*, *CD163*, and *CD11b* expression in hESC-derived macrophages at day 5.

(F) Immunostaining images of day 5 hiPSC-derived macrophages and quantifications for the percentages of marker$^+$ cells among the total number of cells stained by DAPI. n = 5 independent experiments; data are presented as mean ± SD. Scale bar, 50 μm.

See also Figure S1.

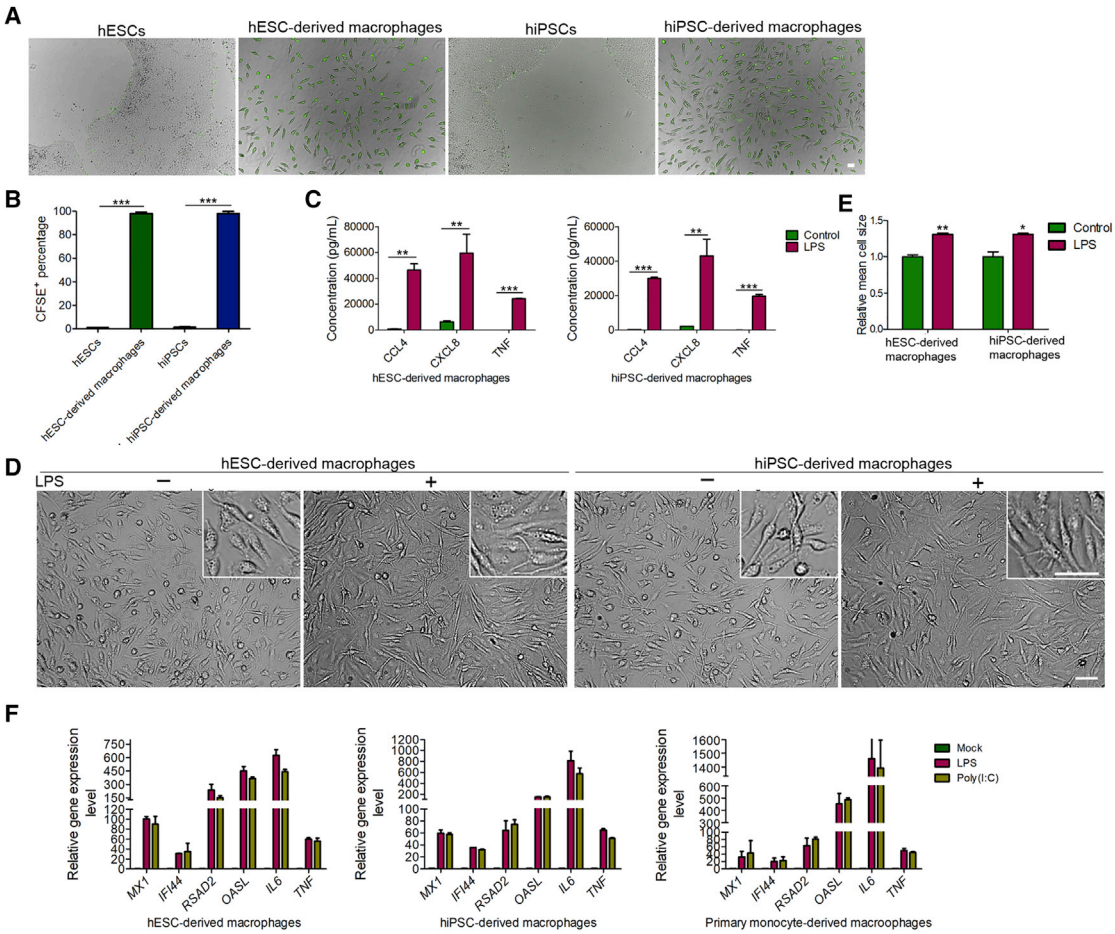

Figure 2. Functional Analysis of Macrophages Derived from Human Pluripotent Stem Cells

(A and B) Images of phagocytosis assay performed with hESCs, hESC-derived macrophages, hiPSCs and hiPSC-derived macrophages incubated with CFSE-labeled myelin debris and quantifications for the percentages of $CFSE^+$ cells among the total cell populations. n = 3 independent experiments; data are presented as mean ± SD; ***p < 0.001; unpaired two-tailed Student's t tests. Scale bar, 50 μm.

(C) ELISA analysis of the secretion of CCL4, CXCL8 and TNF-α from macrophages upon LPS (100 ng/mL) stimulation for 3 hr. n = 3 independent experiments; data are presented as mean ± SD; **p < 0.01; ***p < 0.001; unpaired two-tailed Student's t tests.

(D and E) Phase contrast images of macrophages treated with or without LPS in (C) and quantitative analysis of cell size changes. n = 5 independent experiments; data are presented as mean ± SD; *p < 0.05; **p < 0.01; unpaired two-tailed Student's t tests. Scale bar, 50 μm.

(F) Quantitative analysis of interferon-stimulated genes and pro-inflammatory cytokines gene expression in primary monocyte- and hPSC-derived macrophages after LPS treatment (10 ng/mL) or poly(I:C) transfection (2 μg/mL) using lipofectamine for 12 hr.

See also Figure S1.

assay following infection (Figure 4A). Without infection or LPS treatment, the macrophages migrated into and filled the wound gap within 24 hr after the cells were scraped off. Macrophages that were pre-exposed to ZIKV infection for 4 hr (MOI = 10) similarly migrated into and filled the wound gap within 24 hr, behaving essentially like mock-treated cells. In contrast, DENV-infected macrophages lost the migratory ability under the same conditions, similar to the cells treated with LPS (Figures 4B and 4C), which has been shown to induce macrophage activation and suppress migration (Murray et al., 2014; Mosser and Edwards, 2008; Vereyken et al., 2011; Cougoule et al., 2012). To determine whether the migrating macrophages are infected by ZIKV or represent a bystander population of cells, we examined the macrophages that migrated into the wound gap by immunostaining. As shown in Figure 4B, ZIKV-infected macrophages retained the migratory ability after infection. To rule out cell death as a cause for the failure of DENV-infected cells to fill the gap, we performed terminal deoxynucleotidyl transferase dUTP nick end labeling assay, which confirmed that ZIKV and DENV infection induced apoptosis in less than 6% of the cells at

28 hr post-infection (Figures 4D and 4E), whereas the infection rates and cell viability were around 90% (Figures 4F and 4G).

Distinct Macrophage Migratory Ability Correlates with Differential Induction of MIF Secretion

To explore the mechanism for the different migratory capacities of macrophages infected by ZIKV and DENV, we examined the gene expression profiles in the mock- and virus-infected macrophages12 hr post-infection (Tables S1, S2, S3, S4, S5, and S6). Interestingly, macrophage migration inhibitory factor (MIF), a pivotal regulator of innate immunity and an inhibitor of macrophage migration (Bloom and Bennett, 1966; Calandra and Roger, 2003), was released at a high level from DENV-infected and LPS-treated macrophages (Figure 5A), which is consistent with the previous reports that DENV and LPS can strongly induce MIF expression (Calandra and Roger, 2003; Assunção-Miranda et al., 2010; Chuang et al., 2011), and that LPS inhibits macrophage migration (Vereyken et al., 2011; Cougoule et al., 2012). In contrast, macrophages secreted little MIF after ZIKV infection and mock treatment (Figure 5A). Quantitative gene expression analysis indicated that ZIKV inhibits MIF at the transcription level (Figure 5B). A similar result was also observed in primary monocyte-derived macrophages (Figure S4). To further confirm the role of MIF in macrophage migration, we neutralized MIF in the DENV-infected macrophage cultures with anti-MIF antibody which has been shown to efficiently block the activity of MIF (Hernandez-Pigeon et al., 2007). MIF-neutralizing antibody significantly improved the migratory capacity of DENV-infected macrophages (Figures 5C and 5D). In addition, exogenous MIF treatment of the mock- and $ZIKV^{PR}$-infected macrophages resulted in impaired wound healing (Figures 5C and 5D), consistent with the migration inhibitory role of MIF (Bloom and Bennett, 1966; Calandra and Roger, 2003). MTT assay indicated that MIF does not significantly affect cell viability after 24 hr of treatment (Figure S5). Taken together, these data suggest that different levels of MIF secretion from ZIKV- and DENV-infected macrophages correlate with distinct macrophage migratory abilities.

ZIKV and DENV Infections Induce Different Levels of Cytokine and Chemokine Expression in Macrophages

Considering that MIF is a critical regulator of innate immune and inflammatory responses through the activation of macrophages and T cells and its gene expression is regulated by nuclear factor κB (NF-κB) signaling (Calandra and Roger, 2003; Veillat et al., 2009; Lee et al., 2014; Kim et al., 2017; Chen et al., 2009), we next investigated macrophage immune response to ZIKV and DENV infection. DENV, but not ZIKV, infection dramatically increased RNA levels of pro-inflammatory cytokines and chemokines, including IL-1β (*IL1B*), *IL6*, *TNF*, macrophage inflammatory protein 1α (*MIP1A*/*CCL3*), macrophage inflammatory protein 1 β (*MIP1B*/*CCL4*) and *CXCL8*, in both monocyte- and hPSC-derived macrophages (Figure 6A). On the other hand, both viruses activated interferon-β1(*IFNB1*) expression similarly in each cell type (Figure 6A). In addition, both viruses similarly inhibited interferon-induced transmembrane protein 3 (*IFITM3*) expression in the infected macrophages, while *IFITM3* was highly induced in the uninfected cells by interferon paracrine in the same cell population (Figure S6A), consistent with their ability to block interferon signaling by targeting STAT2 (Ashour et al., 2009; Grant et al., 2016). Further qPCR analysis indicated that other interferon-stimulated genes, including *IFITM1*, *IFIT1*, *MX1*, *IFI44*, and *RSAD2*, were also induced by both viruses in the whole cell population. Type 1 interferons, including *IFNA1* and *IFNA2*, were highly expressed, while type 2 interferon *IFNG*, which is predominantly produced by activated T cells and natural killer cells, was not induced in both virus-infected macrophages (Figure S6B). All these data suggest that the lower pro-inflammatory cytokine/chemokine induction by ZIKV is not a result of general repression of gene activation.

We further validated the differential induction of several well-characterized key pro-inflammatory cytokines (TNF-α and IL-6) and chemokines (CCL4 and CXCL8/IL-8) at the protein level. Significantly higher levels of these cytokines/chemokines were induced by DENV infection, compared with ZIKV, in both monocyte- and hPSC-derived macrophages (Figure 6B), although the infection rates of both viruses were almost the same in each group (Figures S1H, S1I, and S6C).

Given that these pro-inflammatory cytokines and chemokines gene expression are regulated by the NF-κB signaling pathway, we treated ZIKV- and DENV-infected macrophages with or without LPS, a strong activator of NF-κB signaling by binding to CD14 and TLR4 (Zanoni et al., 2011; Murray et al., 2014; Mosser and Edwards, 2008), to further determine whether ZIKV can suppress pro-inflammatory cytokines and chemokines expression through inhibition of the NF-κB signaling pathway. LPS treatment strongly activated expression of IL-6, TNF-α, CCL4, and CXCL8, and viral infections generally interfered with this induction. However, the extent of the suppression was significantly stronger and broader in ZIKV-infected than in DENV-infected cells (Figure 6C), despite similar (~90%) infection rates (Figures S6D and S6E). Taken together, these data suggest that the different abilities of the two viruses to activate the infected macrophages are not due to the difference in interferon production or signaling, but due to the difference in inhibition of the NF-κB signaling pathway.

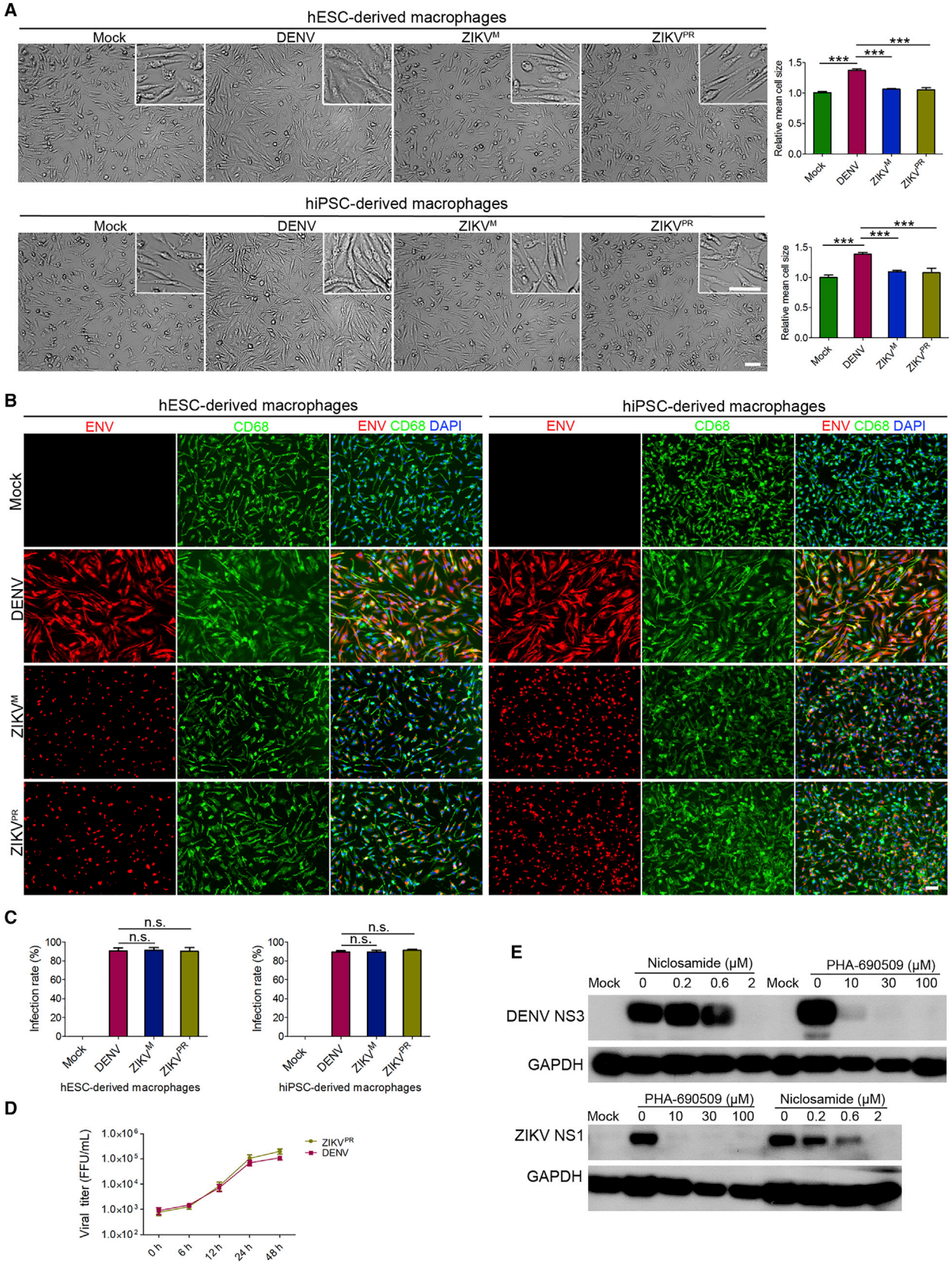

(legend on next page)

ZIKV, but Not DENV, Disrupts the NF-κB-MIF Positive Feedback Loop in the Infected Macrophages

To further verify whether ZIKV can suppress the NF-κB signaling pathway, we utilized an NF-κB luciferase reporter to monitor NF-κB signaling in mock-treated, LPS-treated, or virus-infected macrophages. LPS treatment and DENV infection strongly activated luciferase gene expression (Figure 7A). In contrast, luciferase expression in ZIKV-infected macrophages was at a much lower level (Figure 7A). To further confirm the inhibitory role of ZIKV in the NF-κB signaling pathway activation, we re-stimulated ZIKV- and DENV-infected macrophages with or without LPS. Compared with DENV, ZIKV infection significantly reduced the LPS-induced luciferase expression (Figure 7B), suggesting that ZIKV actively suppresses the activation of the NF-κB signaling pathway. To explore the relationship between the MIF and the NF-κB signaling pathways, we treated macrophages carrying the NF-κB luciferase reporter with human recombinant MIF protein. MIF increased NF-κB induced luciferase expression in a dose-dependent manner (Figure 7C), indicating that MIF has the ability to activate the NF-κB signaling pathway. In addition, treatment of macrophages with TNF-α, a cytokine induced by the NF-κB signaling pathway activation, increased MIF secretion (Figure 7D), consistent with the previous reports that the NF-κB signaling pathway and MIF activate each other, forming a positive feedback loop (Calandra et al., 1994; Kasama et al., 2010; Salminen and Kaarniranta, 2011). Based on these results, we hypothesized that ZIKV-mediated inhibition of NF-κB signaling underlies the mechanism by which ZIKV suppresses MIF production. To test this hypothesis, we treated DENV- and ZIKV-infected macrophages with LPS at 24 hr post-infection. A statistically significant difference was observed for the abilities of the two viruses to suppress LPS-activated MIF production, with ZIKV infection reducing MIF expression much more efficiently (Figure 7E). We next treated DENV- or ZIKV-infected macrophages with MIF to further confirm that ZIKV infection disrupts the NF-κB-MIF positive feedback loop. As shown in Figure 7F, compared with DENV, ZIKV significantly reduced NF-κB activity induced by MIF. Taken together, these data suggest that ZIKV suppresses NF-κB-MIF positive feedback by inhibiting the NF-κB signaling pathway (Figure 7G).

Viruses have developed sophisticated strategies to regulate NF-κB signaling activation by targeting different stages of the signaling cascade from early initiation stage to the final pro-inflammatory genes transcription (Rahman and McFadden, 2011). We found that both DENV and ZIKV infection lead to phosphorylation and translocation of RELA/p65 (Figures S7A and S7B), suggesting that ZIKV may modulate NF-κB activation after RELA/p65 nuclear translocation at the transcription stage. Recently, it has been reported that ZIKV NS5 is able to inhibit the NF-κB signaling pathway (Kumar et al., 2016). Moreover, ZIKV NS5 is mainly localized in the nucleus (Figure S7C). However, further investigations are needed to elucidate the molecular mechanism by which ZIKV regulates the NF-κB signaling pathway.

DISCUSSION

Macrophages are major effector cells in innate and adaptive immunity and play an important role in recognizing and eliminating invading pathogens. After recognition of pathogen-associated molecular patterns, such as LPS and dsRNA, macrophages become activated and secrete a broad array of pro-inflammatory cytokines (e.g., IL-1B, TNF-α, and IL-6) and chemokines (e.g., CCL4 and CXCL8/IL-8) that enhance host immune responses (Murray et al., 2014; Mosser and Edwards, 2008). In the case of DENV infection, a "cytokine storm" formed by pro-inflammatory cytokines and chemokines following infection is a major event of dengue hemorrhagic fever (Halstead, 2007). We observed that both LPS treatment and DENV infection strongly activate pro-inflammatory cytokines and chemokines expression, consistent with the pathogenesis of dengue disease. It has been reported that significantly increased MIF secretion contributes to the severity of DENV infection (Assunção-Miranda et al., 2010). In this

Figure 3. Productive ZIKV and DENV Infection of Human Pluripotent Stem Cell-Derived Macrophages

(A) Phase contrast microscopy images of 2.5 × 10^5 macrophages derived from hESCs and hiPSCs exposed to DENV, $ZIKV^M$, and $ZIKV^{PR}$ (MOI = 10) or mock treated at day 5 for 12 hr and quantitative analysis of cell size change. n = 5 independent experiments; data are presented as mean ± SD; ***p < 0.001; one-way ANOVA. Scale bar, 50 μm.

(B and C) Immunostaining images of cell samples in (A) with virus infection for 24 hr and quantifications for infection rates. n = 5 independent experiments; data are presented as mean ± SD; n.s., not significant; one-way ANOVA. Scale bar, 50 μm.

(D) Virus titers of the supernatants collected from DENV- and $ZIKV^{PR}$-infected macrophages (MOI = 10).

(E) Western blot analysis of the effect of niclosamide and PHA-690509 on ZIKV and $DENV^{PR}$ infection of macrophages at day 5. hiPSC-derived macrophages were treated with niclosamide or PHA-690509 at the indicated concentrations for 1 hr before inoculation with ZIKV and $DENV^{PR}$ (MOI = 10), and cells were harvested at 24 hr after infection for western blot analysis.

See also Figures S1–S3.

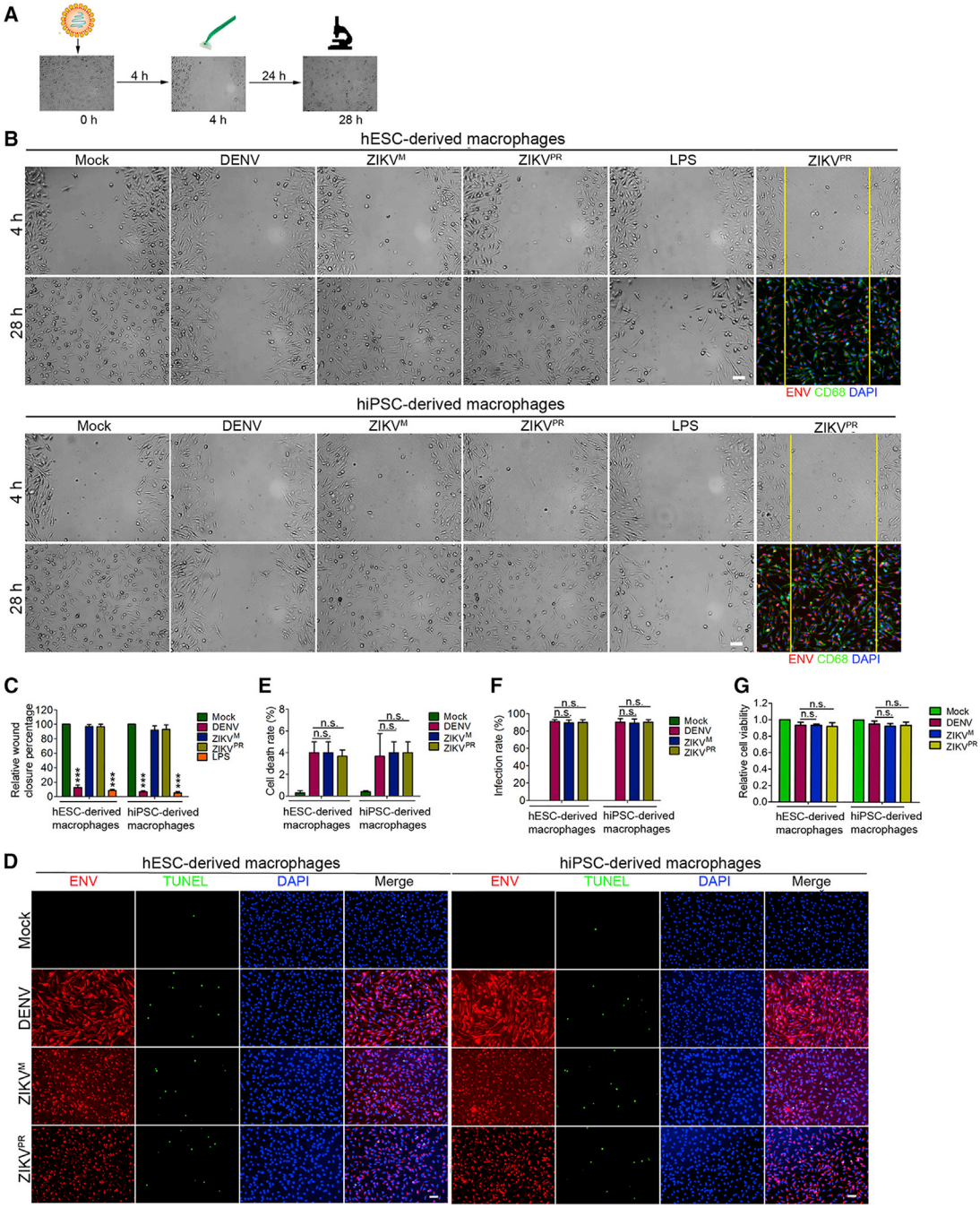

Figure 4. The Impact of ZIKV and DENV Infection on Macrophage Migration

(A) Schematic diagram of wound-healing assay.

(B and C) Phase contrast microscopy and immunostaining images (B) of wound-healing assay performed with DENV-, ZIKV^{M}-, and ZIKV^{PR} infected, LPS (5 ng/mL) or mock-treated day 5 hESC- and hiPSC-derived macrophages showing macrophages migration leading edges immediately after scratching (4 hr post-infection) and after 24 hr (28 hr post-infection) (MOI = 10). Migration ability was quantified by the percentage of wound closure after scratching (C). n = 5 independent experiments; data are presented as mean ± SD; ***p < 0.001; one-way ANOVA. Scale bars, 50 μm.

(D–G) Immunostaining images (D) of macrophage samples in (B) with virus infection for 28 hr and quantifications for cell death rates (E), virus infection rates (F), and relative cell viability (G). n = 5 independent experiments; data are presented as mean ± SD; n.s., not significant; one-way ANOVA. Scale bars, 50 μm.

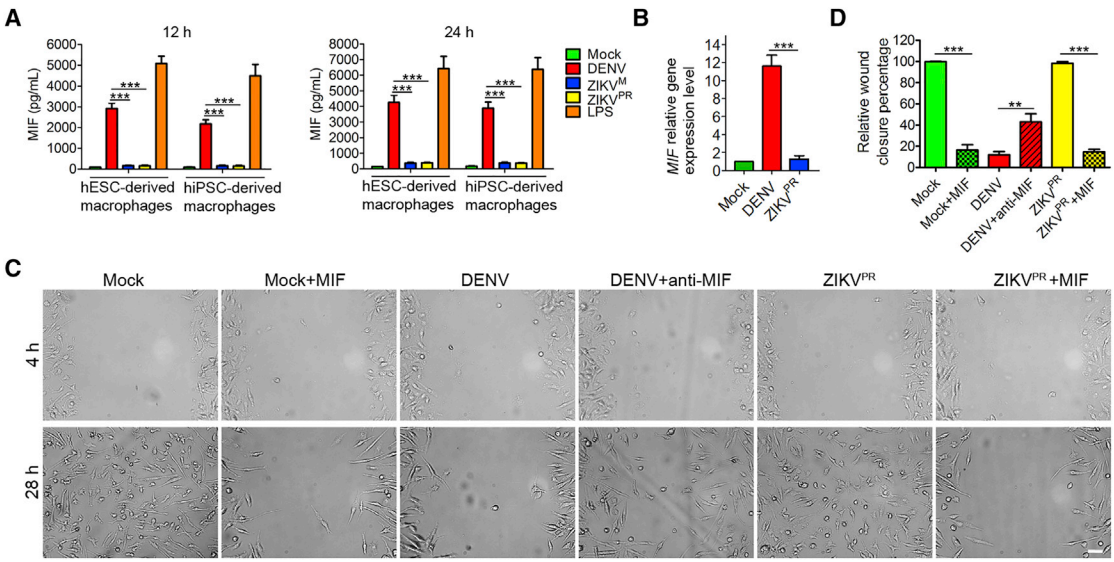

Figure 5. The Effect of MIF on Macrophage Migration

(A) ELISA analysis of the concentrations of MIF in the supernatants collected from DENV-, ZIKV^{M}-, and ZIKV^{PR}-infected, or mock- and LPS (5 ng/mL)-treated macrophage cultures at 12 and 24 hr after scratching in the wound-healing assay (MOI = 10). n = 3 independent experiments; data are presented as mean ± SD; ***p < 0.001; one-way ANOVA.

(B) Quantitative analysis of *MIF* gene expression in the DENV- and ZIKV^{PR}-infected macrophages at 12 hr post-infection. n = 3 independent experiments; data are presented as mean ± SD; ***p < 0.001; one-way ANOVA.

(C and D) Phase contrast microscopy images (C) of wound-healing assay performed with DENV- and ZIKV^{PR}-infected (MOI = 10), or mock-treated macrophages with or without MIF (10 ng/mL), anti-MIF antibody (5 μg/mL) treatment. Cell migration was quantified by the percentage of wound closure after scratching (D). n = 3 independent experiments; data are presented as mean ± SD; **p < 0.01; ***p < 0.001; one-way ANOVA. Scale bar, 50 μm.

See also Figures S4 and S5.

study, we found that MIF production correlates with the inhibition of DENV-infected macrophage migration. While the increased pro-inflammatory cytokines and chemokines promote recruitment and activation of uninfected immune cells to the infection site, it is more advantageous to restrict the migration of DENV-infected macrophages to fight infection locally and limit the virus spread in human tissues. Conversely, ZIKV infection results in little induction of the pro-inflammatory cytokines and chemokines, which leads to a weaker immune response, and prolonged virus infection and persistence in body tissues. In addition, migration of infected macrophages can boost ZIKV's ability to cross physiological barriers and promote virus spread in the body. Of note, we observed that ZIKV only induced minimal cell death in the infected macrophages, which can contribute to its ability to disseminate in patients. In contrast to neural progenitor cells, the low cell death rate was also observed in ZIKV- or DENV-infected primary macrophages, DCs and endothelial cells (Quicke et al., 2016; Mladinich et al., 2017; Bowen et al., 2017; Datan et al., 2016; Schmid and Harris, 2014; Chen and Wang, 2002). The underlying mechanism of differential cell death sensitivity has not been well understood, but may have to do with the unique gene expression profiles in different cell types.

MIF was originally identified as a soluble factor that inhibits the random migration of macrophages and also has tautomerization enzymatic activity (Bloom and Bennett, 1966; Calandra and Roger, 2003), but its migration inhibitor property does not appear to be related to the enzymatic activity (Hermanowski-Vosatka et al., 1999). Although its migration inhibitory activity was reported many years ago, the mechanism for the MIF-induced migration inhibition has not been fully elucidated. MIF mediates its biological activities through different signaling pathways (Calandra and Roger, 2003). These signaling pathways activated by MIF may induce migration inhibition independently of, or combined with, NF-κB signaling activation. In addition, MIF plays a pivotal role in the inflammatory cascade and the innate immune response (Calandra and Roger, 2003). As part of the inflammatory cascade, MIF is rapidly released from virtually all leukocytes, including macrophages, and triggers the release of pro-inflammatory cytokines, including TNF-α, IL-1B, IL-6, and IL-8, via activation of the NF-κB signaling pathway (Calandra and Roger, 2003; Li and Verma, 2002). Many pro-inflammatory cytokines,

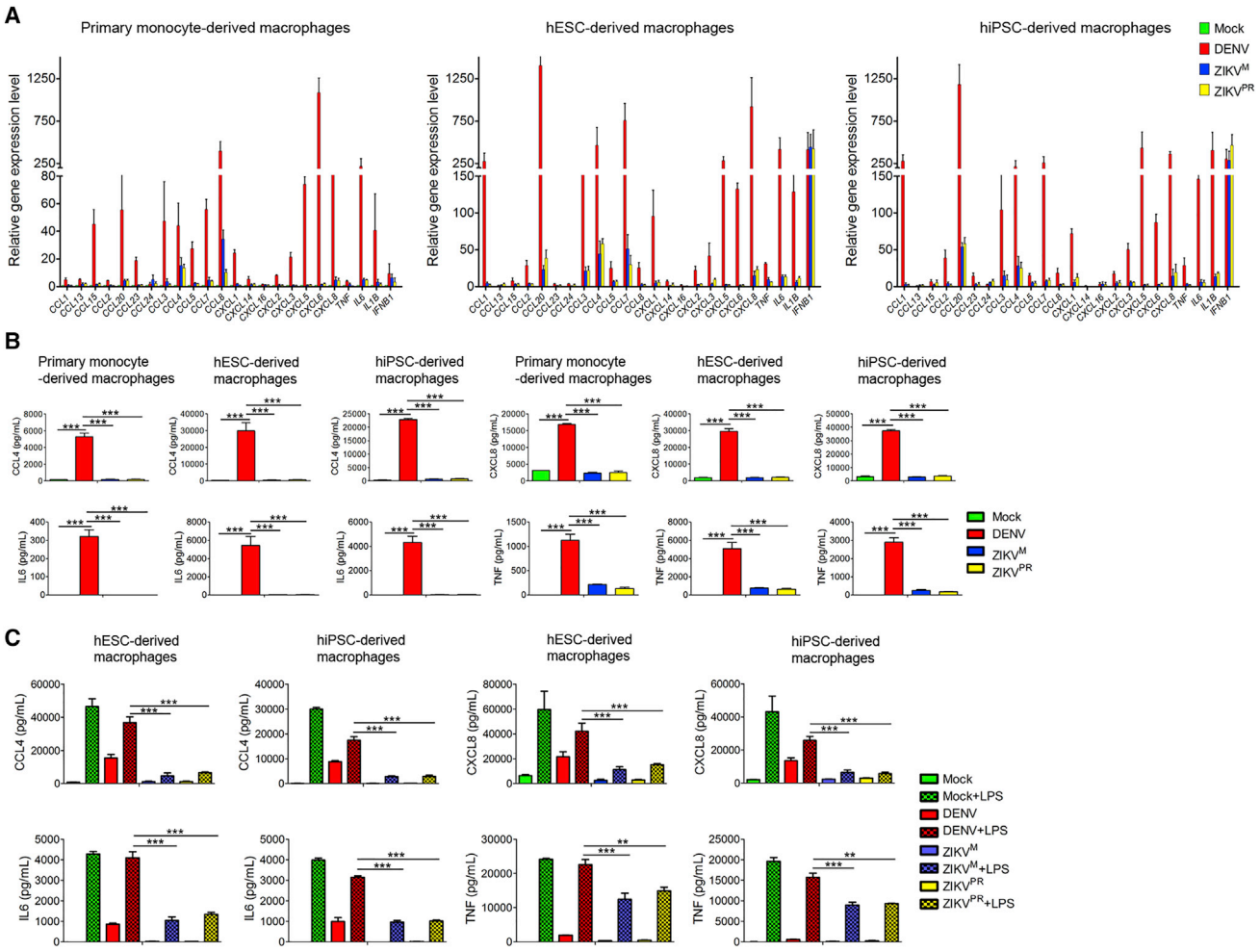

Figure 6. Cytokine and Chemokine Expression in Macrophages Infected with ZIKV and DENV

(A) qPCR analysis of cytokines and chemokines expression in DENV-, ZIKV^{M}-, and ZIKV^{PR}-infected, or mock-treated macrophages derived from primary human monocytes, hESCs or hiPSCs at 12 hr post-infection (MOI = 5). n = 3 independent experiments; data are presented as mean ± SD.

(B) ELISA analysis of the concentrations of CCL4, CXCL8, IL-6, and TNF-α in the supernatants collected from the macrophage cultures at 24 hr post-infection (MOI = 5). n = 3 independent experiments; data are presented as mean ± SD; ***p < 0.001; one-way ANOVA.

(C) ELISA analysis of the concentrations of CCL4, CXCL8, IL-6, and TNF-α in the supernatants collected from macrophage cultures with or without 3 hr of LPS (100 ng/mL) treatment after DENV, ZIKV^{M}, and ZIKV^{PR} infection for 24 hr (MOI = 10). n = 3 independent experiments; data are presented as mean ± SD; **p < 0.01; ***p < 0.001; one-way ANOVA.

See also Figure S6.

such as TNF-α, IL-5, and IL-1B, in turn stimulate *MIF* expression and secretion, forming a positive feedback loop (Calandra et al., 1994; Kasama et al., 2010; Salminen and Kaarniranta, 2011; Arjona et al., 2007; Chen et al., 2015; Veillat et al., 2009; Cao et al., 2005). At the transcriptional level, the 5′ regulatory region of *MIF* gene contains the consensus DNA-binding sequence for NF-κB (Calandra and Roger, 2003), and NF-κB proteins can directly regulate *MIF* gene expression (Veillat et al., 2009; Lee et al., 2014; Kim et al., 2017; Chen et al., 2009). In this study, we found that ZIKV, but not DENV, suppresses pro-inflammatory genes expression by inhibiting the NF-κB signaling pathway, which disrupts the NF-κB-MIF positive feedback loop and leads to the downregulation of MIF production. The MIF inhibition allows ZIKV-infected macrophages to maintain their migratory capacity in a longer time frame post-infection.

In previous studies, many viruses were found to block the NF-κB signaling pathway before RELA/p65 nuclear translocation. However, The E1A protein from human adenovirus

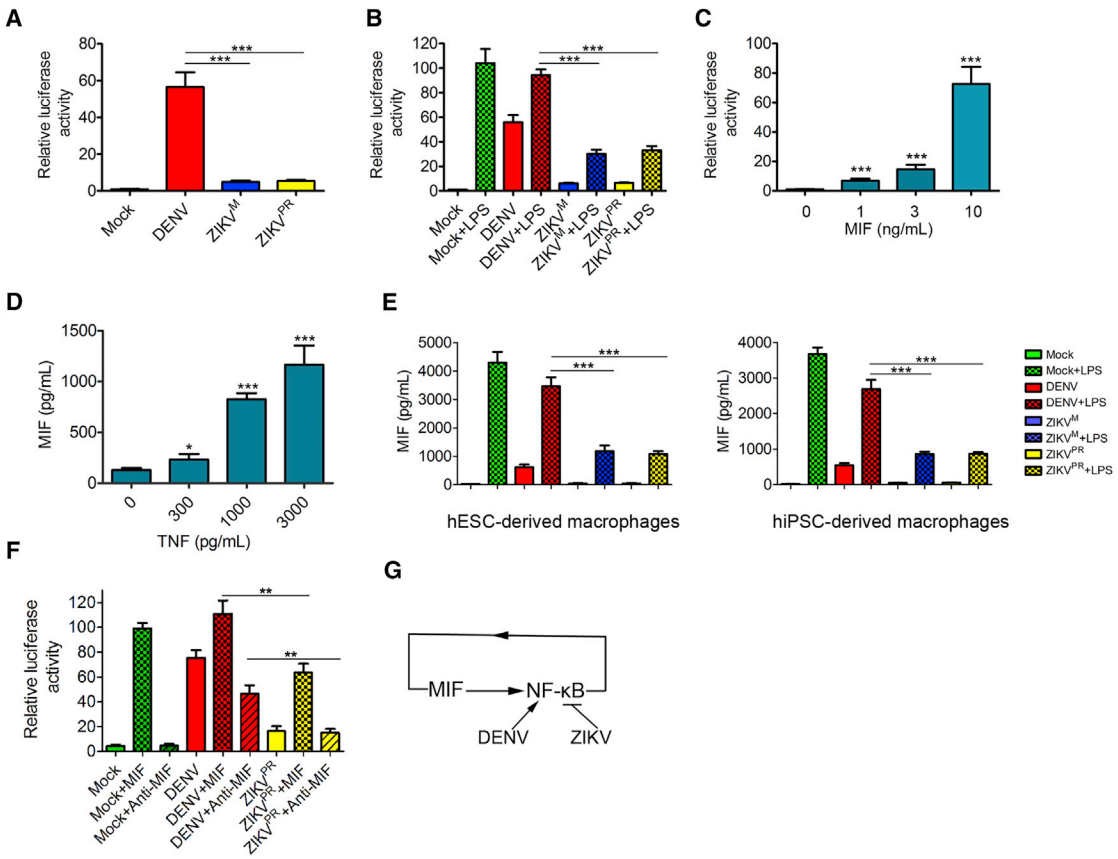

Figure 7. Inhibition of NF-κB-MIF Positive Feedback Loop in Infected Macrophages by ZIKV, but Not DENV

(A) NF-κB luciferase reporter assay showing the relative NF-κB activities in macrophages infected by ZIKV or DENV (MOI = 10) for 24 hr. n = 3 independent experiments; data are presented as mean ± SD; ***p < 0.001; one-way ANOVA.

(B) Relative NF-κB activities in macrophages with or without 3 hr of LPS (100 ng/mL) treatment after DENV, ZIKV^{M}, or ZIKV^{PR} infection for 24 hr (MOI = 10). n = 3 independent experiments; data are presented as mean ± SD; ***p < 0.001; one-way ANOVA.

(C) Relative NF-κB activities in macrophages induced by MIF at the indicated concentrations for 24 hr. n = 3 independent experiments; data are presented as mean ± SD; ***p < 0.001; one-way ANOVA.

(D) ELISA analysis of the concentrations of MIF in the supernatants collected from macrophage cultures treated with TNF-α at the indicated concentrations for 24 hr. n = 3 independent experiments; data are presented as mean ± SD; *p < 0.05; ***p < 0.001; one-way ANOVA.

(E) ELISA analysis of the concentrations of MIF in the supernatants collected from macrophage cultures with or without 3 hr of LPS (100 ng/mL) treatment after DENV, ZIKV^{M}, or ZIKV^{PR} infection for 24 hr (MOI = 10). n = 3 independent experiments; data are presented as mean ± SD; ***p < 0.001; one-way ANOVA.

(F) Relative NF-κB activities in macrophages with or without 24 hr of MIF (20 ng/mL) or anti-MIF antibody (5 μg/mL) treatment at 24 hr post DENV or ZIKV^{PR} infection (MOI = 10). n = 3 independent experiments; data are presented as mean ± SD; **p < 0.01; one-way ANOVA.

(G) A proposed model of inhibition of NF-κB-MIF positive feedback loop by ZIKV. In macrophages, activation of the NF-κB signaling pathway enhances *MIF* expression which in turn further activates NF-κB signaling. ZIKV, but not DENV, disrupts the NF-κB-MIF positive feedback loop, by inhibiting the NF-κB signaling pathway, and decreases MIF production.

See also Figure S7.

12, and NleH1 and NleH2 from *Escherichia coli* O157:H7 str. EDL9883, were reported to suppress NF-κB-dependent transcription at the post-nuclear translocation stage (Rahman and McFadden, 2011). In the case of ZIKV infection, we discovered that RELA/p65 is phosphorylated and translocated to the nucleus after ZIKV infection. Although ZIKV NS5 is mainly localized in the nucleus and has been reported to be able to inhibit NF-κB activity (Kumar et al., 2016), the molecular mechanism by which ZIKV inhibits the NF-κB signaling pathway is still unclear. More efforts need to be made to better understand the pathogenesis of Zika.

In this study, we established a new macrophage model to investigate the yolk sac-derived macrophage-virus interaction. Yolk sac- and monocyte-derived macrophages differ with respect to the developmental origins and the developmental pathways (Varol et al., 2015; Perdiguero and Geissmann, 2016). It has been well documented that, before the establishment of the blood circulation, *Myb*-independent yolk sac progenitor cells give rise to tissue-resident macrophages, such as microglia, Langerhans cells, and Kupffer cells. In adults, yolk sac-derived tissue-resident macrophages are maintained by self-renewal and independent of circulating monocytes throughout adulthood. In contrast, *Myb*-dependent hematopoietic stem cells generate monocytes that give rise to relatively short-lived tissue-resident macrophages in adulthood (Varol et al., 2015; Perdiguero and Geissmann, 2016). In addition to the heterogeneity of macrophage lineage, circulating monocytes are also heterogeneous. Monocytes emerge as a highly plastic and dynamic cellular system in the blood after exiting the bone marrow and can be divided into several subsets based on the differential expression of cellular surface proteins and distinct physiological roles (Gordon and Taylor, 2005). Together, all these increase the heterogeneity of macrophages and may result in the different virus infection efficiencies of monocyte- and yolk sac-derived macrophages.

We produced hPSC-derived macrophages using a protocol developed by Karlsson and coworkers (Karlsson et al., 2008; Panicker et al., 2012; Aflaki et al., 2014), which has recently been shown to produce macrophages in an *MYB*-independent, *RUX1*- and *SPI1* (*PU.1*)-dependent manner, suggesting that these macrophages are derived independent of hematopoietic stem cells and more related to yolk sac-derived tissue macrophages developmentally (Vanhee et al., 2015; Buchrieser et al., 2017; Clarke et al., 2000; Zambidis et al., 2005; Haenseler et al., 2017). Considering that brain microglia are mainly established at the embryo stage (Varol et al., 2015; Perdiguero and Geissmann, 2016), ZIKV-infected microglia may facilitate virus spread in the fetal brain and contribute to fetal microcephaly.

Given the considerable technical challenge of obtaining the yolk sac-derived tissue-resident macrophages, our stem cell-derived macrophage model will be highly valuable for investigating macrophage-pathogen interactions. This macrophage model reveals important features of virus-host interactions that may be associated with the different pathogenesis of dengue and Zika diseases. The ability of this system to model prenatally established macrophages under both physiological and pathological conditions, such as infections and cancer immunity, has significant implications for human diseases research.

EXPERIMENTAL PROCEDURES

Wound-Healing Assay

Wound-healing assays of macrophages with or without virus infection were performed as described previously (Roney et al., 2011). In brief, 3×10^5 macrophages at day 5 were grown on coverslips in 12-well plates before being infected by ZIKV and DENV at an MOI of 10 or treated by 5 ng/mL LPS. At 4 hr post-infection, the cell monolayer was scratched by a sterile micropipette tip, followed by washes with PBS to remove the floating cells. Then the spent medium was put back into each cell sample. The images of the wound-healing process were taken immediately after the scratch, and 24 hr later, to monitor macrophage migration into the gap at ten points per scratch using light microscopy. The wound closure was quantified by measuring the distance covered by the migrated leading edge after scratching using ImageJ. The migratory abilities of macrophages treated by DENV, ZIKV, mock, or LPS were quantified by measuring the percentage of the gap closure in each sample from five independent experiments. For MIF neutralization assay, macrophages were infected by DENV as described above after being treated with 5 μg/mL anti-MIF polyclonal antibody (R&D Systems, catalog no. AF-289) for 30 min. The same amount of goat isotype polyclonal immunoglobulin antibody (Abcam) was used as the control. For MIF inhibition assay, macrophages were infected with or without ZIKV for 60 min before treated with or without 10 ng/mL MIF (R&D Systems, catalog no. 289-MF). At 4 hr post DENV or ZIKV infection, wound-healing assays were performed in all cell cultures as described above.

For detailed information regarding other experimental procedures, please see the Supplemental Experimental Procedures.

Statistical Analysis

Statistical analyses were carried out using GraphPad Prism 5.0 software (GraphPad Software, San Diego, CA). Unless mentioned otherwise, the results shown are representative of three independent experiments. All the data are presented as mean ± SD. The p values were calculated by one-way ANOVA with a Bonferonni test to make multiple pairwise comparisons between different groups or by unpaired two-tailed Student's t tests to compare the mean values of two groups: n.s., not significant; *$p < 0.05$; **$p < 0.01$; ***$p < 0.001$.

ACCESSION NUMBERS

The RNA-seq data have been deposited in the NCBI Sequence Read Archive with the accession numbers: PRJNA368720 and SRP078315.

SUPPLEMENTAL INFORMATION

Supplemental Information includes Supplemental Experimental Procedures, seven figures, and seven tables and can be found with this article online at https://doi.org/10.1016/j.stemcr.2018.06.006.

AUTHOR CONTRIBUTIONS

J.L. and H.T. designed the study and wrote the manuscript. J.L. performed most of the experiments. Y.C. designed the primers and

performed the viral titration experiments. A.R. conducted some of the ELISA analysis. C.H. provided viruses stocks. D.V. and K.K. performed the bioinformatics analyses. J.W. performed the phagocytosis assay. Y.R. provided helpful suggestions for this study and directed the macrophage functional experiments. T.B.M. and C.C. provided essential technical assistance for human macrophage differentiation.

ACKNOWLEDGMENTS

We would like to thank Li Sun, Sarah Ogden, Brian Washburn, Emily Lee, and Kristina Poduch for technical assistance. This study is supported in part by NIH grants U19 AI131130 and R21 AI119530 (to H.T.) and Zika seed funding from Florida State University (to H.T.).

Received: August 21, 2017
Revised: June 4, 2018
Accepted: June 6, 2018
Published: July 5, 2018

REFERENCES

Aflaki, E., Stubblefield, B.K., Maniwang, E., Lopez, G., Moaven, N., Goldin, E., Marugan, J., Patnaik, S., Dutra, A., Southall, N., et al. (2014). Macrophage models of Gaucher disease for evaluating disease pathogenesis and candidate drugs. Sci. Transl. Med. *6*, 240ra273.

Arjona, A., Foellmer, H.G., Town, T., Leng, L., McDonald, C., Wang, T., Wong, S.J., Montgomery, R.R., Fikrig, E., and Bucala, R. (2007). Abrogation of macrophage migration inhibitory factor decreases West Nile virus lethality by limiting viral neuroinvasion. J. Clin. Invest. *117*, 3059–3066.

Ashour, J., Laurent-Rolle, M., Shi, P.Y., and García-Sastre, A. (2009). NS5 of dengue virus mediates STAT2 binding and degradation. J. Virol. *83*, 5408–5418.

Assunção-Miranda, I., Amaral, F.A., Bozza, F.A., Fagundes, C.T., Sousa, L.P., Souza, D.G., Pacheco, P., Barbosa-Lima, G., Gomes, R.N., Bozza, P.T., et al. (2010). Contribution of macrophage migration inhibitory factor to the pathogenesis of dengue virus infection. FASEB J. *24*, 218–228.

Bloom, B.R., and Bennett, B. (1966). Mechanism of a reaction in vitro associated with delayed-type hypersensitivity. Science *153*, 80–82.

Bowen, J.R., Quicke, K.M., Maddur, M.S., O'Neal, J.T., McDonald, C.E., Fedorova, N.B., Puri, V., Shabman, R.S., Pulendran, B., and Suthar, M.S. (2017). Zika virus antagonizes type i interferon responses during infection of human dendritic cells. PLoS Pathog. *13*, e1006164.

Buchrieser, J., James, W., and Moore, M.D. (2017). Human induced pluripotent stem cell-derived macrophages share ontogeny with MYB-independent tissue-resident macrophages. Stem Cell Reports *8*, 1–12.

Calandra, T., and Roger, T. (2003). Macrophage migration inhibitory factor: a regulator of innate immunity. Nat. Rev. Immunol. *3*, 791–800.

Calandra, T., Bernhagen, J., Mitchell, R.A., and Bucala, R. (1994). The macrophage is an important and previously unrecognized source of macrophage migration inhibitory factor. J. Exp. Med. *179*, 1895–1902.

Cao, W.G., Morin, M., Metz, C., Maheux, R., and Akoum, A. (2005). Stimulation of macrophage migration inhibitory factor expression in endometrial stromal cells by interleukin 1,beta involving the nuclear transcription factor NFkappaB. Biol. Reprod. *73*, 565–570.

Castellucci, M., Kosanke, G., Verdenelli, F., Huppertz, B., and Kaufmann, P. (2000). Villous sprouting: fundamental mechanisms of human placental development. Hum. Reprod. Update *6*, 485–494.

Chen, Y.C., and Wang, S.Y. (2002). Activation of terminally differentiated human monocytes/macrophages by dengue virus: productive infection, hierarchical production of innate cytokines and chemokines, and the synergistic effect of lipopolysaccharide. J. Virol. *76*, 9877–9887.

Chen, L., Yang, G., Zhang, X., Wu, J., Gu, Q., Wei, M., Yang, J., Zhu, Y., Wang, N., and Guan, Y. (2009). Induction of MIF expression by oxidized LDL via activation of NF-kappaB in vascular smooth muscle cells. Atherosclerosis *207*, 428–433.

Chen, L., Zhou, X., Fan, L.X., Yao, Y., Swenson-Fields, K.I., Gadjeva, M., Wallace, D.P., Peters, D.J., Yu, A., Grantham, J.J., and Li, X. (2015). Macrophage migration inhibitory factor promotes cyst growth in polycystic kidney disease. J. Clin. Invest. *125*, 2399–2412.

Chuang, Y.C., Lei, H.Y., Liu, H.S., Lin, Y.S., Fu, T.F., and Yeh, T.M. (2011). Macrophage migration inhibitory factor induced by dengue virus infection increases vascular permeability. Cytokine *54*, 222–231.

Clarke, D., Vegiopoulos, A., Crawford, A., Mucenski, M., Bonifer, C., and Frampton, J. (2000). In vitro differentiation of c-myb(–/–) ES cells reveals that the colony forming capacity of unilineage macrophage precursors and myeloid progenitor commitment are c-Myb independent. Oncogene *19*, 3343–3351.

Costa, H., Gouilly, J., Mansuy, J.M., Chen, Q., Levy, C., Cartron, G., Veas, F., Al-Daccak, R., Izopet, J., and Jabrane-Ferrat, N. (2016). Zika virus reveals broad tissue and cell tropism during the first trimester of pregnancy. Sci. Rep. *6*, 35296.

Cougoule, C., Van Goethem, E., Le Cabec, V., Lafouresse, F., Dupré, L., Mehraj, V., Mège, J.L., Lastrucci, C., and Maridonneau-Parini, I. (2012). Blood leukocytes and macrophages of various phenotypes have distinct abilities to form podosomes and to migrate in 3D environments. Eur. J. Cell Biol *91*, 938–949.

Datan, E., Roy, S.G., Germain, G., Zali, N., McLean, J.E., Golshan, G., Harbajan, S., Lockshin, R.A., and Zakeri, Z. (2016). Dengue-induced autophagy, virus replication and protection from cell death require ER stress (PERK) pathway activation. Cell Death Dis. *7*, e2127.

Gordon, S., and Taylor, P.R. (2005). Monocyte and macrophage heterogeneity. Nat. Rev. Immunol. *5*, 953–964.

Govero, J., Esakky, P., Scheaffer, S.M., Fernandez, E., Drury, A., Platt, D.J., Gorman, M.J., Richner, J.M., Caine, E.A., Salazar, V., et al. (2016). Zika virus infection damages the testes in mice. Nature *540*, 438–442.

Grant, A., Ponia, S.S., Tripathi, S., Balasubramaniam, V., Miorin, L., Sourisseau, M., Schwarz, M.C., Sánchez-Seco, M.P., Evans, M.J., Best, S.M., and García-Sastre, A. (2016). Zika virus targets human STAT2 to inhibit type I interferon signaling. Cell Host Microbe *19*, 882–890.

Gustafsson, C., Mjösberg, J., Matussek, A., Geffers, R., Matthiesen, L., Berg, G., Sharma, S., Buer, J., and Ernerudh, J. (2008). Gene expression profiling of human decidual macrophages: evidence for immunosuppressive phenotype. PLoS One *3*, e2078.

Haenseler, W., Sansom, S.N., Buchrieser, J., Newey, S.E., Moore, C.S., Nicholls, F.J., Chintawar, S., Schnell, C., Antel, J.P., Allen, N.D., et al. (2017). A highly efficient human pluripotent stem cell microglia model displays a neuronal-co-culture-specific expression profile and inflammatory response. Stem Cell Reports *8*, 1727–1742.

Halstead, S.B. (2007). Dengue. Lancet *370*, 1644–1652.

Heikkinen, J., Möttönen, M., Komi, J., Alanen, A., and Lassila, O. (2003). Phenotypic characterization of human decidual macrophages. Clin. Exp. Immunol. *131*, 498–505.

Hermanowski-Vosatka, A., Mundt, S.S., Ayala, J.M., Goyal, S., Hanlon, W.A., Czerwinski, R.M., Wright, S.D., and Whitman, C.P. (1999). Enzymatically inactive macrophage migration inhibitory factor inhibits monocyte chemotaxis and random migration. Biochemistry *38*, 12841–12849.

Hernandez-Pigeon, H., Jean, C., Charruyer, A., Haure, M.J., Baudouin, C., Charveron, M., Quillet-Mary, A., and Laurent, G. (2007). UVA induces granzyme B in human keratinocytes through MIF: implication in extracellular matrix remodeling. J. Biol. Chem. *282*, 8157–8164.

Jurado, K.A., Simoni, M.K., Tang, Z., Uraki, R., Hwang, J., Householder, S., Wu, M., Lindenbach, B.D., Abrahams, V.M., Guller, S., and Fikrig, E. (2016). Zika virus productively infects primary human placenta-specific macrophages. JCI Insight *1*. https://doi.org/10.1172/jci.insight.88461.

Karlsson, K.R., Cowley, S., Martinez, F.O., Shaw, M., Minger, S.L., and James, W. (2008). Homogeneous monocytes and macrophages from human embryonic stem cells following coculture-free differentiation in M-CSF and IL-3. Exp. Hematol. *36*, 1167–1175.

Kasama, T., Ohtsuka, K., Sato, M., Takahashi, R., Wakabayashi, K., and Kobayashi, K. (2010). Macrophage migration inhibitory factor: a multifunctional cytokine in rheumatic diseases. Arthritis *2010*, 106202.

Kass, D.E., and Merlino, M. (2016). Zika virus. N. Engl. J. Med. *375*, 294.

Kim, J.H., Lee, J., Bae, S.J., Kim, Y., Park, B.J., Choi, J.W., Kwon, J., Cha, G.H., Yoo, H.J., Jo, E.K., et al. (2017). NADPH oxidase 4 is required for the generation of macrophage migration inhibitory factor and host defense against *Toxoplasma gondii* infection. Sci. Rep. *7*, 6361.

Kumar, A., Hou, S., Airo, A.M., Limonta, D., Mancinelli, V., Branton, W., Power, C., and Hobman, T.C. (2016). Zika virus inhibits type-I interferon production and downstream signaling. EMBO Rep. *17*, 1766–1775.

Lee, S.H., Kim, D.Y., Kang, Y.Y., Kim, H., Jang, J., Lee, M.N., Oh, G.T., Kang, S.W., and Choi, E.Y. (2014). Developmental endothelial locus-1 inhibits MIF production through suppression of NF-κB in macrophages. Int. J. Mol. Med. *33*, 919–924.

Li, Q., and Verma, I.M. (2002). NF-kappaB regulation in the immune system. Nat. Rev. Immunol. *2*, 725–734.

Li, H., Saucedo-Cuevas, L., Regla-Nava, J.A., Chai, G., Sheets, N., Tang, W., Terskikh, A.V., Shresta, S., and Gleeson, J.G. (2016). Zika virus infects neural progenitors in the adult mouse brain and alters proliferation. Cell Stem Cell *19*, 593–598.

Lidstrom, C., Matthiesen, L., Berg, G., Sharma, S., Ernerudh, J., and Ekerfelt, C. (2003). Cytokine secretion patterns of NK cells and macrophages in early human pregnancy decidua and blood: implications for suppressor macrophages in decidua. Am. J. Reprod. Immunol. *50*, 444–452.

Ma, W., Li, S., Ma, S., Jia, L., Zhang, F., Zhang, Y., Zhang, J., Wong, G., Zhang, S., Lu, X., et al. (2016). Zika virus causes testis damage and leads to male infertility in mice. Cell *167*, 1511–1524.e10.

Miner, J.J., and Diamond, M.S. (2017). Zika virus pathogenesis and tissue tropism. Cell Host Microbe *21*, 134–142.

Mladinich, M.C., Schwedes, J., and Mackow, E.R. (2017). Zika virus persistently infects and is basolaterally released from primary human brain microvascular endothelial cells. MBio *8*. https://doi.org/10.1128/mBio.00952-17.

Mlakar, J., Korva, M., Tul, N., Popović, M., Poljšak-Prijatelj, M., Mraz, J., Kolenc, M., Resman Rus, K., Vesnaver Vipotnik, T., Fabjan Vodušek, V., et al. (2016). Zika virus associated with microcephaly. N. Engl. J. Med. *374*, 951–958.

Moreira, J., Peixoto, T.M., Machado de Siqueira, A., and Lamas, C.C. (2017). Sexually acquired Zika virus: a systematic review. Clin. Microbiol. Infect. *23*, 296–305.

Mosser, D.M., and Edwards, J.P. (2008). Exploring the full spectrum of macrophage activation. Nat. Rev. Immunol. *8*, 958–969.

Murray, P.J., Allen, J.E., Biswas, S.K., Fisher, E.A., Gilroy, D.W., Goerdt, S., Gordon, S., Hamilton, J.A., Ivashkiv, L.B., Lawrence, T., et al. (2014). Macrophage activation and polarization: nomenclature and experimental guidelines. Immunity *41*, 14–20.

Panicker, L.M., Miller, D., Park, T.S., Patel, B., Azevedo, J.L., Awad, O., Masood, M.A., Veenstra, T.D., Goldin, E., Stubblefield, B.K., et al. (2012). Induced pluripotent stem cell model recapitulates pathologic hallmarks of Gaucher disease. Proc. Natl. Acad. Sci. USA *109*, 18054–18059.

Perdiguero, E.G., and Geissmann, F. (2016). The development and maintenance of resident macrophages. Nat. Immunol. *17*, 2–8.

Quicke, K.M., Bowen, J.R., Johnson, E.L., McDonald, C.E., Ma, H., O'Neal, J.T., Rajakumar, A., Wrammert, J., Rimawi, B.H., Pulendran, B., et al. (2016). Zika virus infects human placental macrophages. Cell Host Microbe *20*, 83–90.

Rahman, M.M., and McFadden, G. (2011). Modulation of NF-κB signalling by microbial pathogens. Nat. Rev. Microbiol. *9*, 291–306.

Rasmussen, S.A., Jamieson, D.J., Honein, M.A., and Petersen, L.R. (2016). Zika virus and birth defects–reviewing the evidence for causality. N. Engl. J. Med. *374*, 1981–1987.

Roney, K.E., O'Connor, B.P., Wen, H., Holl, E.K., Guthrie, E.H., Davis, B.K., Jones, S.W., Jha, S., Sharek, L., Garcia-Mata, R., et al.

(2011). Plexin-B2 negatively regulates macrophage motility, Rac, and Cdc42 activation. PLoS One *6*, e24795.

Salminen, A., and Kaarniranta, K. (2011). Control of p53 and NF-κB signaling by WIP1 and MIF: role in cellular senescence and organismal aging. Cell. Signal. *23*, 747–752.

Schmid, M.A., and Harris, E. (2014). Monocyte recruitment to the dermis and differentiation to dendritic cells increases the targets for dengue virus replication. PLoS Pathog. *10*, e1004541.

Tang, H., Hammack, C., Ogden, S.C., Wen, Z., Qian, X., Li, Y., Yao, B., Shin, J., Zhang, F., Lee, E.M., et al. (2016). Zika virus infects human cortical neural progenitors and attenuates their growth. Cell Stem Cell *18*, 587–590.

Vanhee, S., De Mulder, K., Van Caeneghem, Y., Verstichel, G., Van Roy, N., Menten, B., Velghe, I., Philippé, J., De Bleser, D., Lambrecht, B.N., et al. (2015). In vitro human embryonic stem cell hematopoiesis mimics MYB-independent yolk sac hematopoiesis. Haematologica *100*, 157–166.

Varol, C., Mildner, A., and Jung, S. (2015). Macrophages: development and tissue specialization. Annu. Rev. Immunol. *33*, 643–675.

Veillat, V., Lavoie, C.H., Metz, C.N., Roger, T., Labelle, Y., and Akoum, A. (2009). Involvement of nuclear factor-kappaB in macrophage migration inhibitory factor gene transcription up-regulation induced by interleukin-1 beta in ectopic endometrial cells. Fertil. Steril. *91*, 2148–2156.

Vereyken, E.J., Heijnen, P.D., Baron, W., de Vries, E.H., Dijkstra, C.D., and Teunissen, C.E. (2011). Classically and alternatively activated bone marrow derived macrophages differ in cytoskeletal functions and migration towards specific CNS cell types. J. Neuroinflammation *8*, 58.

Xu, M., Lee, E.M., Wen, Z., Cheng, Y., Huang, W.K., Qian, X., Tcw, J., Kouznetsova, J., Ogden, S.C., Hammack, C., et al. (2016). Identification of small-molecule inhibitors of Zika virus infection and induced neural cell death via a drug repurposing screen. Nat. Med. *10*, 1101–1107.

Zambidis, E.T., Peault, B., Park, T.S., Bunz, F., and Civin, C.I. (2005). Hematopoietic differentiation of human embryonic stem cells progresses through sequential hematoendothelial, primitive, and definitive stages resembling human yolk sac development. Blood *106*, 860–870.

Zanoni, I., Ostuni, R., Marek, L.R., Barresi, S., Barbalat, R., Barton, G.M., Granucci, F., and Kagan, J.C. (2011). CD14 controls the LPS-induced endocytosis of Toll-like receptor 4. Cell. *147*, 868–880.